Bull. Mater. Sci., Vol. 29, No. 1, February 2006, pp. 35–41 © Indian Academy of Sciences.

Electrical conduction in $(Na_{0.125}Bi_{0.125}Ba_{0.65}Ca_{0.1})(Nd_{0.065}Ti_{0.87}Nb_{0.065})O_3$ ceramic

SYED MAHBOOB, G PRASAD and G S KUMAR*

Department of Physics, Osmania University, Hyderabad 500 007, India

MS received 15 April 2005; revised 10 November 2005

Abstract. Polycrystalline ceramic samples of sodium bismuth titanate with simultaneous doping at A and B sites have been studied for the influence of these dopants on the electrical conduction mechanism. A.C. conductivity measurements were done on the prepared sample in a wide range of frequency and temperature. These studies revealed that the conduction in the sample arises due to hopping of bound charges. Four-term power law is used to characterize the frequency dependence of a.c. conductivity. From the temperature dependence of the exponents, the a.c. conduction in the samples is explained.

Keywords. A.C. studies; oxygen vacancies; translational hopping conduction; reorientational hopping conduction.

1. Introduction

Perovskite type oxides of general formula, ABO_3, are well known for their phase transitions, which strongly affect both the structural and electrical properties. $BaTiO_3$ (BT) is a classical non-relaxor ferroelectric material (Ravez and Simon 2000). It crystallizes in the tetragonal *P*4*mm* space group at room temperature (Kazaoui *et al* 1992) and undergoes a series of phase transitions from rhombohedral to orthorhombic at 183 K, from orthorhombic to tetragonal at 268 K and from tetragonal to cubic at 393 K (Megaw 1945). Homo or heterovalent substitution at either A site or B site or at both sites in $BaTiO_3$ have resulted in relaxor behaviour with the disappearance of intermediate phases (Farhi *et al* 1999; Ravez and Simon 2000). In our earlier studies, we investigated the effect of heterovalent substitution of Nd and Nb at B site in $BaTiO_3$ ($BaNd_xTi_{1-2x}Nb_xO_3$) (Mahboob *et al* 2005a). Dielectric studies revealed that for $x > 0{\cdot}025$ the materials exhibited relaxor behaviour with dielectric maximum temperature (T_{max}) below room temperature. It is reported that the relaxor materials with T_{max} close to room temperature will exhibit good electrostrictive properties. Our aim to prepare a good relaxor material with T_{max} close to room temperature was not fulfilled, because for higher compositions ($x = 0{\cdot}1$, $0{\cdot}2$), though good relaxor behaviour was observed, T_{max} are very low, < 170 K, and for lower compositions ($x = 0{\cdot}05$, $0{\cdot}025$), though the T_{max} is close to room temperature, the degree of relaxor behaviour was low.

$Na_{0.5}Bi_{0.5}TiO_3$ (NBT) is a disordered ABO_3 type perovskite material with rhombohedral symmetry at room temperature. It undergoes a series of phase transitions: (i) ferroelectric rhombohedral to antiferroelectric tetragonal around 230°C, (ii) antiferroelectric tetragonal to non polar tetragonal around 320°C and (iii) nonpolar tetragonal to cubic around 520°C (Takenaka *et al* 1990).

NBT is also considered to be an excellent candidate to be lead free piezoelectric ceramics due to properties of strong ferroelectricity with relatively large remanent polarization, $P_r = 38$ μC/cm and a large coercive field, $E_c = 73$ kV/cm (Smolensky *et al* 1961). However, it is difficult to pole because of its high coercive field and relatively large conductivity. Therefore, NBT based solid solutions were studied in order to resolve this problem. Several solid solutions of NBT with $PbTiO_3$ (Sakata *et al* 1992), $SrTiO_3$ (Sakata and Masuda 1974; Takenaka and Sakata 1989), $CaTiO_3$ (Takenaka *et al* 1989), $BaTiO_3$ (Takenaka *et al* 1991; Chiang *et al* 1998; Li *et al* 2003; Wang *et al* 2003), $Na_{0.5}Bi_{0.5}TiO_3$–$BaZrO_3$ (Sossits *et al* 2001) and $Na_{0.5}Bi_{0.5}TiO_3$–$BaZrO_3$–$CaTiO_3$ (Ravez *et al* 1999) etc have been studied. Among these NBT based systems, $Na_{0.5}Bi_{0.5}TiO_3$–$BaTiO_3$, $Na_{0.5}Bi_{0.5}TiO_3$–$BaZrO_3$ and $Na_{0.5}Bi_{0.5}TiO_3$–$BaZrO_3$–$CaTiO_3$ are more interesting with respect to their dielectric and piezoelectric/electrostrictive properties. Hence, $Na_{0.5}Bi_{0.5}TiO_3$ (NBT) and $CaTiO_3$ (CT) were selected to improve the dielectric relaxor properties of $BaNd_{0.1}Ti_{0.8}Nb_{0.1}O_3$ and to shift the T_{max} towards room temperature.

$(Na_{0.125}Bi_{0.125}Ba_{0.65}Ca_{0.1})(Nd_{0.065}Ti_{0.87}Nb_{0.065})O_3$ is a novel composition obtained from the miscible solid solution of $Na_{0.5}Bi_{0.5}TiO_3$, $Ba(Nd_{0.1}Ti_{0.8}Nb_{0.1})O_3$ and $CaTiO_3$. In our previous studies, we investigated the dielectric relaxation behaviour of this ternary system in the low temperature regime, 80–300 K and impedance relaxation in the high temperature regime, 673–900 K (Mahboob *et al* 2005b).

*Author for correspondence (gskumar1948@sify.com)

Based on the values of activation energy obtained for relaxation, the high temperature relaxation was attributed to the relaxation of hopping species via dipole formation and the asymmetry in the Z', Z'' vs temperature curves (Z' and Z'' are real and imaginary parts of complex impedance, Z^*, and are defined as $Z' = |Z^*|\cos(q)$, $Z'' = |Z^*|\sin(q)$, where q is phase angle) was attributed to the type of conduction mechanism. In order to separate out different types of conduction mechanism a detailed analysis of a.c. conductivity data is required.

In the present work, a.c. conductivity studies have been performed extensively on $(Na_{0\cdot125}Bi_{0\cdot125}Ba_{0\cdot65}Ca_{0\cdot1})$ $(Nd_{0\cdot065}Ti_{0\cdot87}Nb_{0\cdot065})O_3$ over a wide range of temperature and frequency. Based on the results obtained, the experimental data are analysed and the conduction mechanism in the present sample explained.

2. Experimental

Ceramic composition, $(Na_{0\cdot125}Bi_{0\cdot125}Ba_{0\cdot65}Ca_{0\cdot1})$ $(Nd_{0\cdot065}Ti_{0\cdot87}Nb_{0\cdot065})O_3$, was prepared by solid state sintering route, using stoichiometric mixture of high purity initial reagents $BaCO_3$, TiO_2, Nd_2O_3, Nb_2O_5, $CaCO_3$, Na_2CO_3 and Bi_2O_3. The stoichiometric mixture was calcined at 925°C for 5 h. The calcined powder was ground, mixed and pressed in the form of ceramic discs of 10 mm diameter and 1–2 mm thickness. These ceramic discs were finally sintered at 1190°C for 4 h. X-ray diffraction pattern was recorded using PW3040/60 X'pert PRO X-ray powder diffractometer.

The ceramic samples were polished to obtain flat surface and then the flat surface of the samples were electroded using silver paint by firing at 400 K for 20 min. D.C. conductivity measurements on this electroded sample were made using Keithley 617 programmable electrometer as function of temperature (300–900 K). AUTOLAB PGSTAT 30 low frequency impedance analyser was used to carry out impedance/admittance measurements on the ceramic disc as a function of frequency (100 Hz–1 MHz) and in the temperature range (300–900 K).

3. Results and discussion

X-ray diffraction studies revealed single-phase formation with cubic symmetry with lattice parameter, 4·002 Å and the density of the ceramic sample was found to be 94·80% of the theoretical density (Mahboob *et al* 2005).

The Arrhenius plots of d.c. conductivity are shown in figure 1. It can be seen from the plots that the conductivity increases with increase in temperature and changes by about six to seven orders of magnitude in the temperature range investigated. The rise in conductivity may be due to thermally generated carriers in the sample, and hence Arrhenius type conduction becomes apparent. A change in the slope of the Arrhenius plots was observed. It is reported that slight change in slopes is related to transition temperatures

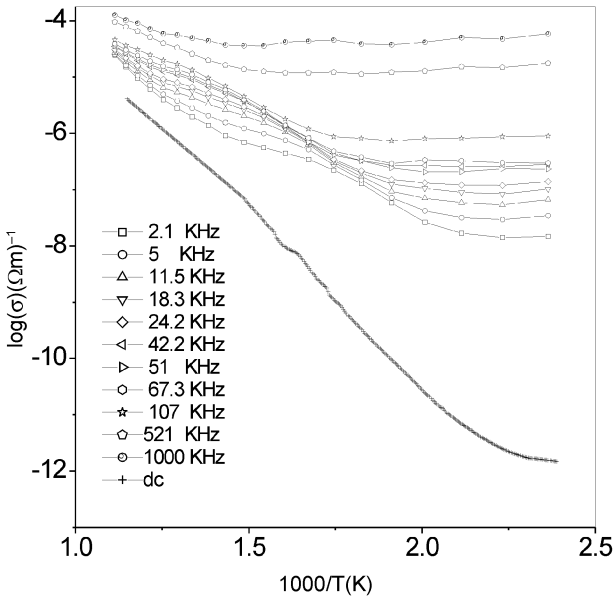

Figure 1. log (s) vs 1000/T(K) at different frequencies.

(Prasad 2000). But in our case the samples are cubic at room temperature and hence a phase transition is not expected. The slight changes in slopes may be due to contributions from different regions in polycrystalline materials (i.e. from grain, grain boundary etc), where, appearance (disappearance) of space charge polarization takes place accompanied with the change in activation energy. These changes can also be related to change in conduction mechanism. The activation energy values are calculated from the slope of Arrhenius plots by fitting the experimental data to the Arrhenius relation

$$s_{dc} = s_0 \exp(-E/kT), \tag{1}$$

where E is the activation energy, k the Boltzmann's constant, s_0 a constant and T the temperature in Kelvin. The values obtained from fitting are tabulated in table 1.

In the present study, the a.c. conductivity of the samples were determined from the real part of the admittance (via impedance measurements), using the relation

$$s' = (Y' * t)/A', \tag{2}$$

where t and A' are thickness and area of the sample, respectively.

Arrhenius a.c. conductivity plots of log (s') vs 1000/T(K) at different frequencies are shown in figure 1. The frequency dependence of a.c. conductivity may arise due to free as well as bound carriers. If the conduction is due to free carriers then the conductivity must decrease with increase in frequency (Kamalasanan *et al* 1993). In the present case, a.c. conductivity increases with increasing frequency and therefore, the observed a.c. conductivity must be related to the bound carriers trapped in the sample. It is observed from these plots (figure 1) that in low temperature regime, a.c. conductivity increased with increase in frequency

Table 1. Activation energy values for d.c. and a.c. conductivities

	DC conductivity Activation energy (eV)	AC conductivity activation energy (eV)			
		11·5 KHz		18·3 KHz	
Sample	Temperature range (K)	Temperature range (K)		Temperature range (K)	
	525–890	590–725	770–898	590–725	770–898
NBC	1·317	0·475	0·884	0·431	0·709

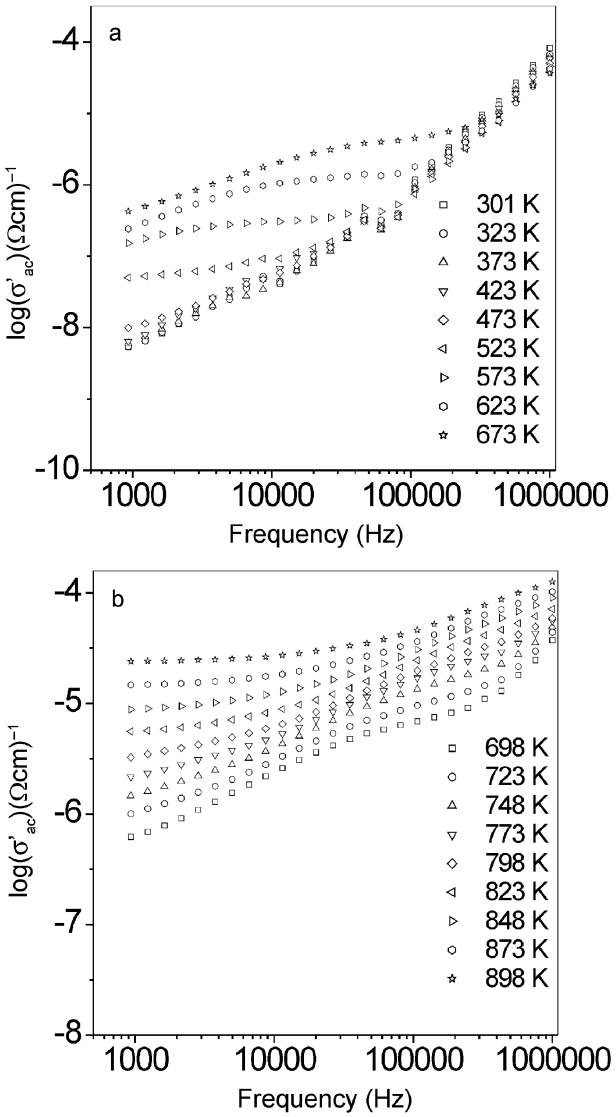

Figure 2. (**a**, **b**). $\log(s'_{a.c.})$ vs frequency (Hz) at different constant temperatures.

indicating dispersion of conductivity with frequency. With increase in temperature dispersion in conductivity narrowed and all the curves for different frequencies appeared to merge into single curve at high temperatures. It has also been observed that the d.c. conductivity of the sample at lower temperature region is few orders of magnitude less than the a.c. conductivity and its variation with temperature is also different. This is not unusual because the d.c. conductivity is determined by the most difficult transition in complete percolation paths between the electrodes, while the a.c. conductivity is determined by the easiest local movement of the charges. Thus, it is natural to expect that absolute magnitude of these two parameters may not be closely related, and it is evident that their temperature dependence is completely different.

The activation energy for d.c. and a.c. conductivities in different temperature regions was obtained from the slope of curve of Arrhenius plots (figure 1). The activation energy values are found to increase with the increase in temperature as shown in table 1. It is observed that the activation energy values for a.c. conductivity is less than that for d.c. conductivity. It is also observed that a.c. activation energy calculated at high frequency is lower than that at low frequency. This is due to the fact that at low frequencies the overall conductivity is due to the mobility/transportation of charge carriers over long distance rather than relaxation/orientational mechanism, in which case charge mobility/transportation is restricted to only the nearest neighbouring lattice sites (Dyre and Thomas 2000). Since the energy required for the relaxation/orientational process is lower than that required for mobility of charge carriers over a long distance, hence the observed greater activation energy for conduction at lower frequency than for higher frequency.

A convenient formalism to investigate the frequency dependence of conductivity in a variety of materials is based on the power law relation proposed by Jonscher (1983),

$$s'(w) = s(0) + Aw^s, \tag{3}$$

where $s'(w)$ is the total conductivity, $s(0)$ the frequency independent conductivity, and the coefficient A and exponent s are temperature and material dependent. The term Aw^s contains the a.c. dependence and characterizes all dispersion phenomena. The exponent s has been found to behave in a variety of forms (Elliot 1987; Funke 1993; Upadhyay *et al* 1998), a constant, decreasing with temperature, increasing with temperature, etc but always varying within $0 < s < 1$.

However, in general, the frequency dependence of conductivity do not follow the simple power relation as given above but follows according to double power law (Funke 1993; Pelaiz-Barranco *et al* 1998)

$$s'(w) = s_0 + B_1 w^{s_1} + B_2 w^{s_2}. \tag{4}$$

The exponent, $0 < s_1 < 1$, characterizes the low frequency region, corresponding to translational ion hopping. The exponent, $0 < s_2 < 2$, characterizes the high frequency region, indicating the existence of well localized relaxation/ reorientational process (Ahmed 2002), the activation energy of which is ascribed to reorientation ionic hopping.

It is observed from figure 2(a, b), that log(s) vs w does not follow either the simple power law relation given in (3) or the double power law relation (4). In the measured frequency range, four slopes are observed in the temperature regime (723–848 K). In the entire frequency range investigated the conductivity does not vary considerably with temperature from 300–473 K. With increase of temperature from 477–673 K, strong dispersion in conductivity with temperature was observed in the low frequency regime (500 Hz–100 KHz), whereas smaller dispersion in conductivity with temperature in the high frequency regime (100 KHz–1 MHz) was observed. With further increase of temperature from 673–898 K, strong dispersion in conductivity with temperature was observed in the entire frequency range investigated.

It is also observed that dispersion of conductivity with frequency decreases in the low frequency regime (1–100 KHz) with increase of temperature from 698–898 K and becomes a plateau type region at higher temperatures associated with the term, s_0, showing little dispersion with frequency. This is due to the fact that intrinsic conductivity is dominant at low frequency regime at higher temperatures. The a.c. conductivity in the low frequency regime 500 Hz–5 KHz is characterized by a flat response with nearly equal slopes for $T \geqslant 823$ K.

In the jump relaxation model (JRM) introduced by Funke (1993) to account for ionic conduction in solids, there is a high probability for a jumping ion to jump back (unsuccessful hop). However, if the neighbourhood becomes relaxed with respect to the ion's position, the ion stays in the new site. The conductivity in the low frequency region is associated with successful hops. Beyond the low frequency region many hops are unsuccessful, and as the frequency increases, more hops are unsuccessful. The change in the ratio of successful to unsuccessful hops results in dispersive conductivity. The JRM suggests that different activation energies are associated with unsuccessful and successful hopping processes.

The frequency and temperature dependence of a.c. conductivity resembles that of hopping type conduction. We now analyse our results in terms of hopping conduction.

Applying JRM to the frequency response of the conductivity for the present material, it was possible to fit the data to a quadruple (four term) power law as given below. Figure 3 shows the log ($s'_{\text{a.c.}}$) vs frequency showing four different regions and the lines are linear fit to data in different regions using quadruple (four-term) power law

$$s'_{\text{a.c.}} = B_1 w^{s_1} + B_2 w^{s_2} + B_3 w^{s_3} + B_4 w^{s_4}.$$

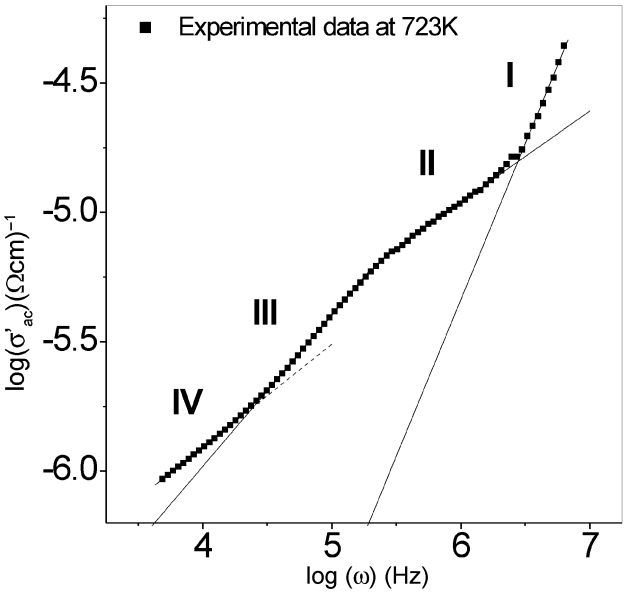

Figure 3. log($s'_{\text{a.c.}}$) vs log(w) curves showing linear fitting using four term power law in different frequency regions.

The frequency corresponding to the point of intersection of tangents drawn to the log($s'_{\text{a.c.}}$) vs log(w) curves in regions II and I is designated as w_{p12} (figure 3). Similarly the frequency corresponding to the point of intersection of tangents drawn to the log($s'_{\text{a.c.}}$) vs log(w) curves in regions IV and III is designated as w_{p34}. It was found that the values of s_1 (in the high frequency region) are always more than s_2, s_3, s_4 in the temperature range investigated. The variation of temperature dependent exponents (s_1, s_2, s_3, s_4), and relaxation frequency (w_{p12}, w_{p34}) are plotted as a function of 1000/T(K) as shown in figure 4. The frequency range in which the exponents (s_1, s_2, s_3, s_4) are evaluated at different temperatures are summarized in table 2. With increase in temperature, the value of s_1 decreases and approaches zero at much high temperatures thereby indicating that d.c. conductivity dominates at higher temperatures. The fact that the values of s_2, s_3, s_4 are less than 0·5 in the temperature regime investigated and their temperature dependence over a wide range of temperature studied indicates that the conduction mechanism in these materials is not due to the intrinsic polarization process, and can be associated with the hopping of charged species across the charged defects (Kim and Kim 2000).

As in the case of ionic crystals, in the perovskite ceramic materials there is a possibility of Schottky and Frenkel defects and the ions may move between lattice points (i.e. interstitial points for Frenkel defect) and also by jumping over unoccupied points (for Schottky defects). Movements of lattice ions at higher temperature may also lead to conductivity in the present samples. Hence, in the present case, the frequency response of the conductivity is interpreted in terms of the jump relaxation model, where the conduction is due to translational and localized orientational hopping. The translational hopping gives the long-

Table 2. Frequency range in which a.c. conductivity parameters are evaluated.

Temperature (*K*)	Frequency range (Hz)			
	Region I	Region II	Region III	Region IV
573	9,11,200–2,05,700	15,200–8,698	1,485–774.3	–
598	9,11,200–2,05,700	20,090–8,698	1,485–774.3	–
623	9,11,200–2,05,700	29,150–9,546	3,430–774.3	–
648	9,11,200–2,05,700	29,150–11,500	3,430–774.3	–
673	9,11,200–2,05,700	31,990–13,850	3,430–774.3	–
698	9,11,200–2,05,700	97,700–38,540	16,680–3,765	1,123–774.3
723	9,11,200–4,75,100	2,05,700–55,910	16,680–3,765	1,485–774.3
748	9,11,200–4,75,100	2,05,700–81,110	22,050–4,977	1,963–774.3
773	9,11,200–4,75,100	2,05,700–81,110	31,990–7,925	3,430–774.3
798	9,11,200–4,75,100	2,05,700–81,110	31,990–18,310	3,430–774.3
823	9,11,200–4,75,100	3,27,500–1,29,300	1,07,200–35,110	5,462–774.3
848	–	–	9,11,200–29,180	5,462–774.3
873	–	–	9,11,200–29,180	11,500–774.3

range electrical transport (i.e. d.c. conductivity) in the limit of very long times, i.e. as the frequency approaches zero. Since, $0 < s_2 < 1$, $0 < s_3 < 1$, $0 < s_4 < 1$ and $0 < s_1 < 2$, the conductivity at low frequency may be attributed to the short range translational hopping and the conductivity at higher frequencies may be attributed to the localized orientational back and forth hopping at adjacent lattice sites.

In the perovskite type oxide materials, presence of charge traps in the band gap of the insulator is expected. The oxygen vacancies are one kind of charge trap; the other charge traps may include interface charges, polarization charges, etc. So the above-mentioned hopping type conduction between these trap centres seems a possibility in our case also. The hopping mechanism that generally comes into play in the present samples can be explained as follows:

With the replacement of Ti^{+4} ion with Nd^{+3} and Nb^{+5} ions at lattice site B and replacement of Ba^{+2} ion with Na^{+}, Bi^{+3} and Ca^{+2} ions at lattice site A, there is a strong possibility of creation of localized oxygen vacancies (as illustrated below). These oxygen vacancies are created in order to maintain localized charge neutrality because of different valence states of the ions that are occupying the lattice sites A and B. In the present perovskite material, (Na^{+}, Bi^{+3}, Ca^{+2}, Ba^{+2}) ions occupy the lattice site A and (Nd^{+3}, Ti^{+4}, Nb^{+5}) ions occupy the lattice site B.

$$BaO + TiO_2 \rightarrow Ba + Ti + 3O,$$

$$6BaO + 3Nd_2O_3 \rightarrow 6Ba + 6Nd_{Ti} + 15O + 3V_O,$$

$$5BaO + 2Nb_2O_5 \rightarrow 5Ba + 4Nb_{Ti} + 15O + V_{Ti},$$

$$Bi_2O_3 + 3TiO_2 \rightarrow 2Bi_{Ba} + 3Ti + 9O + V_{Ba},$$

$$3Na_2O + 6TiO_2 \rightarrow 6Na_{Ba} + 6Ti + 15O + 3V_O,$$

$$CaO + TiO_2 \rightarrow Ca + Ti + 3O.$$

By combining the above equations we get

$$12BaO + 11TiO_2 + 3Nd_2O_3 + 2Nb_2O_5 + Bi_2O_3 + 3Na_2O + CaO \rightarrow 12Ba + 11Ti + 6Nd_{Ti} + 4Nb_{Ti} + 6Na_{Ba} + Ca_{Ba} + 2Bi_{Ba} + V_{Ba} + V_{Ti} + 6V_O + 60O,$$

where Nd_{Ti} represents the incorporation of Nd at Ti position, Nb_{Ti} represents the incorporation of Nb at Ti position, Na_{Ba} represents incorporation of Na at Ba position, Ca_{Ba} represents incorporation of Ca at Ba position, Bi_{Ba} represents incorporation of Bi at Ba position, V_{Ti} represents the titanium vacancy, V_{Ba} represents the Ba vacancy and V_O represents the oxygen vacancy.

In the present investigation, the ceramic samples have been sintered at high temperatures, > 1100°C, a slight amount of oxygen loss occurs according to the Kroger-Vink (1956) notation and Prasad (2000)

$$V_O \rightarrow V_O + e',$$

$$V_O \rightarrow V_O'' + e'',$$

where V_O is the oxygen vacancy, V_O' and V_O'' are single and double ionized oxygen vacancies, respectively and e' the electron released or captured. Since Nb can exist in +3 and +5 states and Ti can exist in +3 and +4 states, there is a possibility that the electrons released in the above reaction may be captured by Nb^{+5} or Ti^{+4} to generate Nb^{+3} or Ti^{+3}. Capture/release of electron by Nd^{+3}, Na^{+1} can be ruled out as Nd^{+3}, Na^{+1} have stable states, +3, +1, respectively. Thus there is a possibility of conduction arising due to the hopping of electrons among Nb^{+5} and Nb^{+3} and Ti^{+4} and Ti^{+3}. At low frequencies conductivity may arise due to short range translational hopping of electrons among Nb^{+5} and Nb^{+3} and Ti^{+4} and Ti^{+3}. At high frequencies, the conductivity arising due to the localized orientational hopping is dominant (i.e. back and forth hopping of electrons) among Nb^{+5} and Nb^{+3} and Ti^{+4} and Ti^{+3} states.

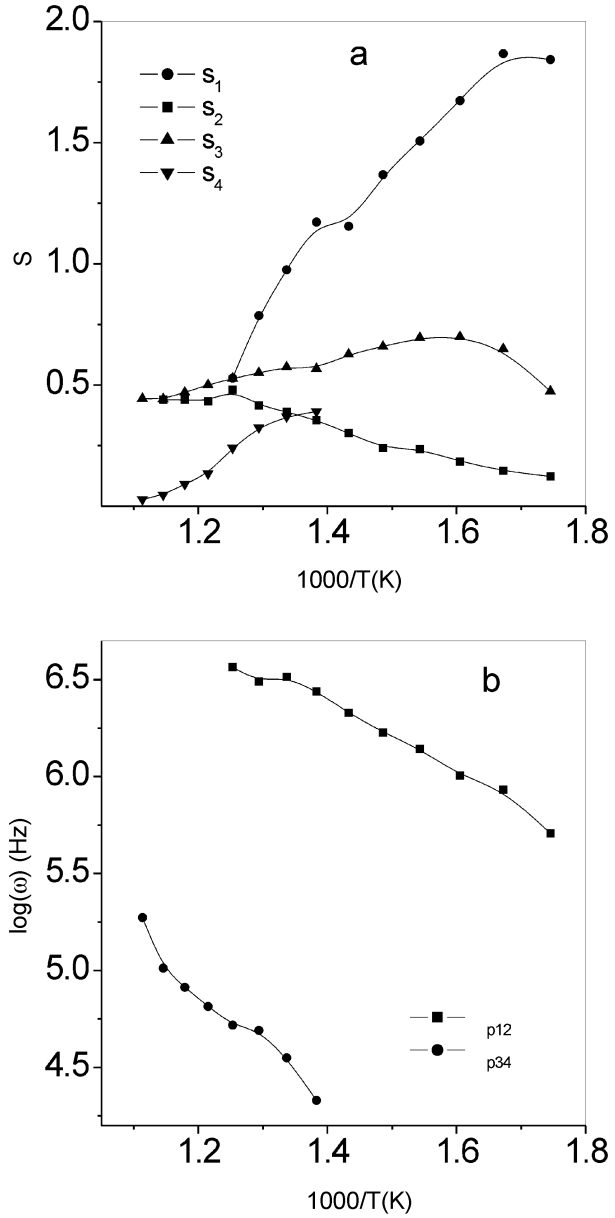

Figure 4. Variation of a.c. conductivity parameters **a**. (s_1, s_2, s_3, s_4) with 1000/T(K) and **b**. log(w) with 1000/T(K).

Since different hopping mechanisms have been reported by different researchers (Funke 1993; Upadhyay *et al* 1998) and these mechanisms predict different temperature and frequency dependencies of the exponent, s: (i) in the case of small polaron hopping, s increases with temperature and decreases with frequency, (ii) while for a large polaron hopping mechanism, s decreases with increasing temperature and frequency and (iii) for quantum mechanical tunneling, s is independent of temperature and decreases with increasing frequency.

One more possibility is that ions, Nb^{+3} and Ti^{+3}, at lattice sites may form dipoles with vacant oxygen sites, V_O and V_O'', respectively. These dipoles can change their orientation by electron hopping. Therefore, in the measured temperature region, the observed exponential dependence of a.c. conductivity, s_1, in the high frequency region shows that conduction occurs by process (ii), i.e. as a result of the excitation of charge carriers at the conduction band edge and hopping at energies close to it. Nb^{+3} and V_O'' and Ti^{+3} and V_O' give rise to localized energy levels in the energy gap of $(Na_{0\cdot125}Bi_{0\cdot125}\ Ba_{0\cdot65}Ca_{0\cdot1})\ (Nd_{0\cdot065}Ti_{0\cdot87}\ Nb_{0\cdot065})O_3$. The charge carriers trapped at these localized sites may form large polarons and the conduction occurs as a result of thermally activated large polarons. This is also clear from the temperature dependence of s_1, which decreases with increasing temperature.

Similarly the exponents, s_3, s_4, obtained from the slopes in the low frequency region (regions III and IV) decreases with increase in temperature in the high temperature region indicating conduction occurs by large polaron hopping mechanism and since these are found to be $< 0{\cdot}5$, hence the conduction arises due to short range translation hopping via large polarons.

It is also observed that in the high temperature region, the exponent, s_2, increases with increase in temperature indicating that conduction in region II arises due to the translational hopping via small polaron.

The activation energies calculated from the Arrhenius plots of relaxation frequency (figure 4b) are found to be of the order of $Ew_{p12} = 0{\cdot}377$ eV and $Ew_{p34} = 0{\cdot}455$ eV. These low values of activation energies also confirm that the conduction is due to hopping mechanism.

4. Conclusions

(I) Analysis of a.c. conductivity data reveals that the conductivity is due to hopping mechanism.
(II) The best fit of the conductivity in the entire frequency range is obtained using a four-term power law dependence of frequency. The exponents, $0 < s_2 < 1$, $0 < s_3 < 1$ and $0 < s_4 < 1$, characterizes the intermediate and low frequency regions (regions II, III and IV), corresponding to short range translational hopping. The exponent, $0 < s_1 < 2$, indicates the relaxation/reorientation hopping mechanism in the high frequency region (region I).
(III) The temperature dependence of s_1, s_3 and s_4 indicates the hopping is via large polarons and that of s_2 indicates hopping is via small polarons.

Acknowledgement

The authors would like to thank DRDO, Delhi, for financial support.

References

Ahmed A A Youssef 2002 *Z. Naturforsch.* **57a** 263
Chiang Yet Ming, Gregory W Farrey and Andrey N Soukhojak 1998 *Appl. Phys. Lett.* **73** N25 3683

Dyre Jeppe C and Thomas B S 2000 *Rev. Mod. Phys.* **72** 873
Elliot S R 1987 *Adv. Phys.* **36** 135
Farhi R, Marssi M El, Simon A and Ravez J 1999 *Eur. Phys. J.* **B9** 599
Funke K 1993 *Prog. Solid State Chem.* **22** 111
Jonscher A K 1983 *Dielectric relaxation in solids* (London: Chelsea Dielectrics Press)
Kamalasanan M N, Deepak Kumar N and Chandra S 1993 *J. Appl. Phys.* **74** 5679
Kazaoui S, Ravez J, Elissalde C and Maglione M 1992 *Ferroelectrics* **135** 85
Kim J S and Kim J N 2000 *Jpn. J. Appl. Phys.* **39** 3502
Kroger F A and Vink H 1956 *J. Solid State Phys.* **3** 307
Li Hui-Dong, Chu-De Feng and Ping Hua Xiang 2003 *Jpn. J. Appl. Phys.* **42** 7387
Mahboob Syed, Dutta A B, Swaminathan G, Prasad G and Kumar G S 2005a *Ferroelectrics* **326** 79
Mahboob Syed, Prasad G and Kumar G S 2005b *Mater. Chem. & Phys.* (in press)
Megaw H D 1945 *Nature* **154** 484
Pelaiz-Barranco A, Gutierrez-Amador M P, Huanosta A and Valenzuela R 1998 *Appl. Phys. Lett.* **73** 2039
Prasad N V 2000 *Studies on rare earth substituted bismuth layered structure ferroelectromagnetic ceramics*, Ph D Thesis, Osmania University, Hyderabad
Ravez J and Simon A 2000 *Eur. Phys. J. AP* **11** 9
Ravez J, Broustera Cedric and Simon A 1999 *J. Mater. Chem.* **9** 1609
Sakata K and Masuda Y 1974 *Ferroelectrics* **5** 347
Sakata K, Takenaka T and Naitou Y 1992 *Ferroelectrics* **131** 219
Smolensky G, Isupov V A, Agranovskaya A I and Krainik N N 1961 *Sov. Phys. Solid State* **2** 2651
Sossits A Sheets, Andrey N Soukhojak, Naoki Ohashi and Yet-Ming Chiang 2001 *J. Appl. Phys.* **90** 5287
Takenaka T and Sakata K 1989 *Ferroelectrics* **95** 153
Takenaka T, Sakata K and Toda K 1989 *Jpn J. Appl. Phys.* **28** 59
Takenaka T, Sakata K and Toda K 1990 *Ferroelectrics* **106** 375
Takenaka T, Maruyama K and Sakata K 1991 *Jpn J. Appl. Phys.* **30** 2236
Upadhyay Shail, Sahu Ashok Kumar, Devender Kumar and Om Parkash 1998 *J. Appl. Phys.* **84** 828
Wang Xiaoxing, Helen Lai-Wa Chan and Chung Loong Choy 2003 *Solid State Commun.* **125** 395